

Optimal thermal bath for robust excitation energy transfer in disordered light-harvesting complex 2 of purple bacteria

This content has been downloaded from IOPscience. Please scroll down to see the full text.

2013 New J. Phys. 15 125030

(<http://iopscience.iop.org/1367-2630/15/12/125030>)

View [the table of contents for this issue](#), or go to the [journal homepage](#) for more

Download details:

IP Address: 174.25.38.220

This content was downloaded on 25/12/2013 at 04:36

Please note that [terms and conditions apply](#).

Optimal thermal bath for robust excitation energy transfer in disordered light-harvesting complex 2 of purple bacteria

Liam Cleary and Jianshu Cao¹

Department of Chemistry, Massachusetts Institute of Technology, Cambridge, MA 02139, USA

E-mail: jianshu@mit.edu

New Journal of Physics **15** (2013) 125030 (13pp)

Received 16 August 2013

Published 23 December 2013

Online at <http://www.njp.org/>

doi:10.1088/1367-2630/15/12/125030

Abstract. The existence of an optimal thermal bath to facilitate robust energy transfer between the spectrally separated B800 and B850 rings in light-harvesting complex 2 (LH2) of purple bacteria is investigated via the multichromophoric Förster theory. Due to the inherent energy bias between the two rings, the energy transfer rate from B800 to B850 is maximized as a function of the bath coupling strength, establishing an optimization criterion. Critically, upon inclusion of energetic disorder, this maximum is averaged out. However, noting the distribution of transfer rates, we find that the bath coupling strength can yield a minimal dispersion for the rate distribution, i.e. a maximum ratio of mean to standard deviation, thus achieving maximum energy transfer robust to the effects of static disorder.

¹ Author to whom any correspondence should be addressed.



Content from this work may be used under the terms of the [Creative Commons Attribution 3.0 licence](https://creativecommons.org/licenses/by/3.0/). Any further distribution of this work must maintain attribution to the author(s) and the title of the work, journal citation and DOI.

Contents

1. Theory	3
1.1. Generalized Förster resonance energy transfer rate	3
1.2. Light-harvesting complex 2 (LH2) of purple bacteria	5
2. Results	7
3. Conclusions	9
Acknowledgments	10
Appendix A. LH2 model calculation details	10
Appendix B. Slow and fast bath dynamics	11
References	12

Quantum transport in a noisy, disordered system is of fundamental interest in condensed matter physics, and is ubiquitous in solid state, semiconductor, chemical and biological physics. In the latter most, much effort has recently focused on understanding the remarkably high efficiency of excitation energy transfer (EET) processes in photosynthetic pigment–protein complexes [1–6]. Significantly, this high efficiency is achieved in the presence of an inherently noisy and disordered environment and over many different length and time scales. The strength of the noise may vary from weak to strong, but often is comparable to the intrasystem electronic coupling strengths, so that over the course of the EET the exciton motion ranges from largely coherent to completely incoherent [7, 8]. The presence of disorder furthermore, either in the electronic coupling (structural) or site energies (energetic), can dramatically alter the energy landscape and thus the EET dynamics. In order to fully understand the design principles of the pigment–protein complex, disorder must be included in the optimization of the coherent and incoherent quantum dynamics with respect to the interaction with the protein environment. The establishment of optimal design principles for efficient EET in these natural complexes can have direct implications for the design of efficient synthetic devices [9–12].

The B800 and B850 rings of light-harvesting complex 2 (LH2) in purple bacteria provide a perfect pigment–protein complex for studying the interplay of coherent and incoherent exciton motion [13, 14]. Here, the pigments of the B800 ring essentially behave as monomers so that its intraring exciton motion is incoherent, while the pigments of the B850 ring are strongly electronically coupled, so that its intraring exciton motion is coherent. The B850 ring of LH2 also possesses a high degree of structural N -fold symmetry and consequently eigenstate degeneracy (promoting exciton delocalization) [12, 15–17], so that the presence of energetic disorder (which promotes exciton localization) markedly affects its coherent intraring dynamics. Consideration of energetic static disorder in LH2 is thus crucial to answering the question of an optimal thermal bath in the B800–B850 EET process. Optimization of the EET process with respect to the bath interaction has to date been considered primarily for pigment–protein complexes with little-to-no structural symmetry so that inclusion of disorder is not crucial [18–21].

An appropriate theory for describing the B800–B850 EET is multichromophoric Förster resonance energy transfer (MC-FRET) [22–24], where the MC system is partitioned into a molecular complex with strong intracomplex coupling (donor complex) weakly coupled

to a second molecular complex with strong intracomplex coupling (acceptor complex). The MC-FRET theory then provides a description of the intercomplex EET rate while correctly accounting for the intracomplex electronic coupling. Furthermore, provided the *intercomplex* electronic coupling is weak enough, the theory is valid for a wide range of the bath coupling (noise) strength. Application of the MC-FRET theory however, poses the formidable problem of solving the emission and absorption density operators of a *multichromophoric* complex [25, 26]. Here the presence of both intracomplex electronic coupling and system–bath coupling ultimately requires a perturbative treatment of either coupling for practical solution (in contrast to the single-chromophore FRET, where the donor-emission and acceptor-absorption operators of the single chromophores can be solved systematically, by virtue of the cumulant expansion technique [27]). For example, in a previous application of MC-FRET to B800–B850 EET, Mukai *et al* [28], while solving the diagonal approximation of the MC-FRET, calculate the Green’s function’s self-energy via a second order perturbation in the system–bath coupling. Similarly, in a study of the energetic optimization of B800–B850 EET, Jang *et al* [29], while solving the MC-FRET, employ a quantum master equation valid to second order in the system–bath coupling. In both applications, the bath coupling strength must remain weak relative to the intracomplex electronic coupling. To overcome this difficulty, we utilize a simple, non-perturbative method for calculating the MC-FRET rate, based on the diagonal approximation in the eigenstate basis and the assumption that the eigenstate bath coupling is directly proportional to its inverse participation ratio (IPR). This IPR MC-FRET approach, which is non-perturbative in the bath coupling strength, allows one to interpolate approximately between the weak and strong bath coupling regimes. Furthermore, its computational simplicity allows us to easily study the disordered transfer rate and its distribution over the full range of bath coupling of LH2. The reliability of the approximations involved in the IPR MC-FRET and proposed methods to improve upon its accuracy are presented in [30, 31].

In this work, we report the existence of a maximum relative dispersity (i.e. ratio of mean to standard deviation or signal-to-noise ratio (SNR)) for the distribution of transfer rates between the B800 and B850 rings in LH2 as a function of the bath coupling strength, allowing for robust EET in the presence of energetic static disorder. At room temperature, in the absence of disorder an optimal coupling strength is easily identifiable due to the appearance of a well-defined maximum rate at an intermediate value of the coupling. Upon inclusion of disorder however, whereby this maximum is averaged out, we must extend our optimization criterion to include the dispersion of the distribution of transfer rates, whence an intermediate coupling strength may still be considered optimal as it yields a minimal dispersion, i.e. maximal transfer rate and minimal deviation, thus achieving efficient EET robust to the effects of static disorder.

1. Theory

1.1. Generalized Förster resonance energy transfer rate

Assuming that the electronic coupling J between the donor (D) and acceptor (A) systems is weak and that the donor and acceptor thermal environments are statistically independent, the EET rate is given by the MC-FRET rate [22, 24]

$$k = \sum_{m,m'}^{N_D} \sum_{n,n'}^{N_A} \frac{J_{m,n} J_{m',n'}}{2\pi \hbar^2} \int_{-\infty}^{\infty} E_{m',m}^D(\omega) I_{n,n'}^A(\omega) d\omega, \quad (1)$$

where N_D and N_A are the number of donor and acceptor chromophores respectively, J_{mn} is the intercomplex electronic coupling between donor site m and acceptor site n , $E_{m',m}^D(\omega)$ and $I_{n,n'}^A(\omega)$ are the site basis elements of the donor emission and acceptor absorption density operators via $E_{m',m}^D(\omega) = \langle m'|E_D(\omega)|m\rangle$ and $I_{n,n'}^A(\omega) = \langle n|I_A(\omega)|n'\rangle$. Calculation of the MC-FRET rate can be greatly simplified by assuming that the donor emission and acceptor absorption density operators are diagonal in their respective eigenstate bases, viz.

$$\begin{aligned}\langle \mu|E_D(\omega)|\mu'\rangle &\approx E_\mu^D(\omega)\delta_{\mu,\mu'}, \\ \langle \nu|I_A(\omega)|\nu'\rangle &\approx I_\nu^A(\omega)\delta_{\nu,\nu'},\end{aligned}\quad (2)$$

where $E_\mu^D(\omega)$ and $I_\nu^A(\omega)$ are the diagonal elements of the emission and absorption density operators in the eigenstate basis. Transforming the basis in equation (1), $|m\rangle = \sum_\mu^{N_D} C_\mu^m |\mu\rangle$ and $|n\rangle = \sum_\nu^{N_A} C_\nu^n |\nu\rangle$, and substituting equations (2), we have the diagonal (secular) MC Förster rate

$$k = \sum_{\mu=1}^{N_D} \sum_{\nu=1}^{N_A} \frac{|J_{\mu,\nu}|^2}{2\pi\hbar^2} \int_{-\infty}^{\infty} E_\mu^D(\omega) I_\nu^A(\omega) d\omega \quad (3)$$

often referred to as the generalized Förster rate or the diagonal approximation of MC-FRET, where C_μ^m and C_ν^n are the donor and acceptor eigenstate coefficients, respectively, and we have introduced the eigenstate electronic coupling

$$J_{\mu,\nu} = \sum_{m=1}^{N_D} \sum_{n=1}^{N_A} J_{m,n} C_\mu^m C_\nu^{n*}.$$

EET now occurs via an effective dipolar coupling $J_{\mu,\nu}$ between pairs of donor and acceptor eigenstates $|\mu\rangle$ and $|\nu\rangle$. The diagonal MC-FRET (3) has previously, successfully been applied to EET in LH2 [24, 28].

In order to evaluate the overlap integral in equation (3), we recall that the intracomplex electronic coupling reduces the lineshape of each individual excitonic transition, so that the spectrum of a multichromophoric complex may be approximated by a weighted sum of the eigenstate spectra with their lineshape functions scaled by their corresponding eigenstate participation ratios [32]. This approximation, where the appearance of the IPR is a natural outcome of the unitary transformation to the eigenstate basis, is often used in the calculation of spectroscopic lineshapes for its simplicity. Hence, in addition to using the diagonal approximation equation (3), we adopt the following expressions for the emission and absorption spectra

$$E_\mu^D(\omega) \approx \rho_\mu^{\text{st}} 2\Re \int_0^\infty dt e^{i\omega t} e^{-i(\varepsilon_\mu - N_\mu^D \lambda)t/\hbar - N_\mu^D g^*(t)} \quad (4)$$

and

$$I_\nu^A(\omega) \approx 2\Re \int_0^\infty dt e^{i\omega t} e^{-i(\varepsilon_\nu + N_\nu^A \lambda)t/\hbar - N_\nu^A g(t)}, \quad (5)$$

where $g(t) = \int_0^t dt' \int_0^{t'} dt'' C(t'')$ is the lineshape function of a single chromophore (monomer) and $C(t)$ is the bath correlation function. Here ε_μ and ε_ν are the eigenenergies and $N_\mu^D = \sum_{m=1}^{N_D} |C_\mu^m|^4$ and $N_\nu^A = \sum_{n=1}^{N_A} |C_\nu^n|^4$ are the participation ratios of the donor and acceptor complexes respectively, so that the magnitude of the lineshape function of the μ th/ ν th exciton

is inversely proportional to the extent of its delocalization, i.e. its IPR. The weighting factor appearing in equation (4) is simply the μ th eigenstate population of the donor complex

$$\rho_{\mu}^{\text{st}} = e^{-\beta\varepsilon_{\mu}} / \sum_i e^{-\beta\varepsilon_i}.$$

Finally, both equations (4) and (5) satisfy the normalization conditions $\int_{-\infty}^{\infty} \text{Tr}_{\text{s,D}}\{E^{\text{D}}(\omega)\}d\omega = 1$ and $\int_{-\infty}^{\infty} \text{Tr}_{\text{s,A}}\{I^{\text{A}}(\omega)\}d\omega = N_{\text{A}}$, where $\text{Tr}_{\text{s,D/A}}$ is the trace over the donor/acceptor system degrees of freedom and the integrands are the emission and absorption density of states, respectively. Equation (3) combined with equations (4) and (5) constitute the IPR MC-FRET approximation, which we now apply to the B800–B850 EET in disordered LH2.

1.2. Light-harvesting complex 2 (LH2) of purple bacteria

An immense literature exists on the structure and dynamics of light-harvesting complexes based on an effective Hamiltonian where each bacteriochlorophyll (BChl) molecule of the complex is modeled by a two-level system describing its $S_0 \rightarrow S_1$ transition (the Q_y transition) [33]. Here we study the LH2 of *Rhodospseudomonas acidophila*, (PDB ID code 1NKZ) [34], where, due to the monomeric structure of the B800 ring, we model the donor complex with a single chromophore with a site energy of $E_{\text{D}} = 12\,465 \text{ cm}^{-1}$, so that $N_{\text{D}} = N_{\mu}^{\text{D}} = \rho_{\mu}^{\text{st}} = 1$, in which case the emission spectrum equation (4) becomes the exact monomer spectrum (the spectral calculation is that of a two-level system [27]). This approach to modeling the B800 ring in calculating the B800–B850 EET is successfully used in [23, 28, 29]. The possible role of nearest-neighbor coherence in LH2 B800 is discussed in the conclusion section, and is in general consistent with the calculation without such coherence. To construct the effective Hamiltonian of the B850 ring we use the details presented in [35], where the site energies of the two BChls in the basic $\alpha\beta$ -heterodimer subunit are $E_{2n-1} = 12\,406 \text{ cm}^{-1}$ and $E_{2n} = 12\,602 \text{ cm}^{-1}$ ($n = 1, \dots, 9$), the intradimer coupling is $J_{2n-1,2n} = J_{2n,2n-1} = 363 \text{ cm}^{-1}$ ($n = 1, \dots, 9$) and the interdimer coupling is $J_{2n+1,2n} = J_{2n,2n+1} = J_{1,18} = J_{18,1} = 320 \text{ cm}^{-1}$ ($n = 1, \dots, 8$). The intercomplex B800–B850 electronic couplings J_{mn} are obtained from a point dipole approximation assuming a transition dipole strength of 6.1 D, yielding a largest coupling of 25 cm^{-1} .

While no direct information on the form and magnitude of the bath spectral density of LH2 is yet available, several works have investigated the related B777 and B820 pigment–protein complexes [36–38], revealing a broad bath spectral density with maximum peaks estimated around 180 and 100 cm^{-1} for B777 and B820 respectively. Here, for the specific description of the continuum of harmonic oscillators comprising the donor and acceptor baths we use the form of the Drude–Lorentz spectral density, $\hbar J(\omega) = 2\lambda\Lambda\omega/(\omega^2 + \Lambda^2)$, where λ is the site reorganization energy (bath coupling strength) and Λ is the Debye angular frequency (inverse of the bath correlation time). The bath correlation function is simply [39]

$$C(t) = \int_0^{\infty} d\omega J(\omega) [\coth(\beta\hbar\omega/2) \cos \omega t - i \sin \omega t], \quad (6)$$

where we have assumed independent, identical baths at each site. Further details are presented in appendix A. The above bath description contains the well-known limits of slow and fast bath dynamics, corresponding to inhomogeneous and homogeneous broadening, respectively [27]. A particularly nice result emerges when we consider the corresponding IPR MC-FRET transfer

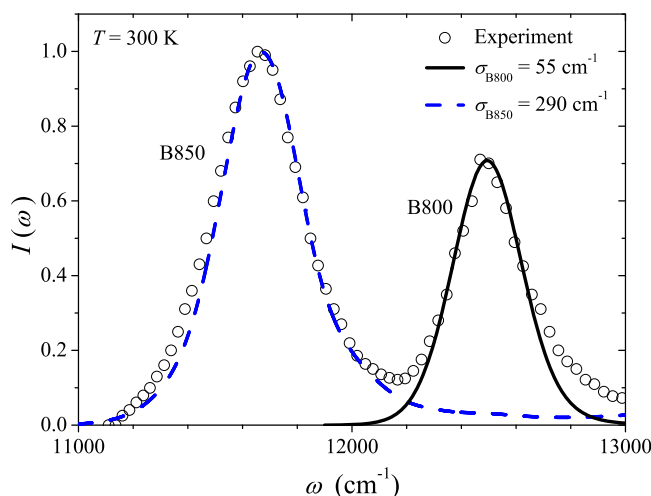


Figure 1. Comparison of the experimental absorption spectrum [40] (open circles) and the calculated B800 (solid line) and B850 (dashed line) absorption spectra at $T = 300$ K. The B800 fit is obtained for an energetic disorder of $\sigma_{B800} = 55$ cm^{-1} and reorganization energy of $\lambda_{B800} = 40$ cm^{-1} , while the B850 fit is obtained for $\sigma_{B850} = 290$ and $\lambda_{B850} = 200$ cm^{-1} .

rates, which yield expressions formally identical to the Marcus rate of electron transfer and the inverse lifetime of the Haken–Strobl model, respectively, with the bath coupling strength scaled by the sum of the participation ratios. We present this result in appendix B for the high temperature approximation of $g(t)$, where simple analytical expressions can be obtained in both limits. Here, however we set the bath angular frequency to $\Lambda = 0.01$ fs^{-1} , an intermediate value of physiological relevance to pigment–protein complexes, where neither the slow nor fast bath dynamics limit is applicable.

In the presence of energetic static disorder, due to protein structural dynamics that occur on a time scale much longer than the excitation dynamics, the site transition energies are modulated so that $E_{m/n} \rightarrow E_{m/n} + \delta E_{m/n}$, where we assume that $\delta E_{m/n}$ are independent Gaussian random variables with zero mean and standard deviations $\sigma_m = \sigma_D$ ($m = 1$) and $\sigma_n = \sigma$ ($n = 1 \dots 18$). In order to establish the bath coupling and disorder strengths in our model at $T = 300$ K, we calculate the B800 and B850 absorption spectra. The MC B850 spectrum is calculated viz.

$$I(\omega) = \left\langle \sum_{v=1}^{N_A} |\vec{d}_v|^2 I_v^A(\omega) \right\rangle, \quad (7)$$

where $\vec{d}_v = \langle 0 | \vec{d} | v \rangle$ is the exciton transition dipole moment, $I_v^A(\omega)$ is given by equation (5), and $\langle \dots \rangle$ indicates averaging over the disorder (achieved by numerically averaging over 10 000 realizations of the spectrum as a function of ω). $|0\rangle$ is the ground state and represents the vacuum state of excitons.

In figure 1, comparison of the spectra with experimental results [40] is presented. The spectrum fits for B800 (solid line) and B850 (dashed line) are obtained for $\sigma_{B800} = 55$ and $\lambda_{B800} = 40$ cm^{-1} , and $\sigma_{B850} = 290$ and $\lambda_{B850} = 200$ cm^{-1} , respectively. These parameters are in good agreement with previous calculations of the B850 linear absorption spectrum using the exact hierarchy method [41] and yield an average transfer rate of $\langle k \rangle = 0.7$ ps^{-1} , in reasonable

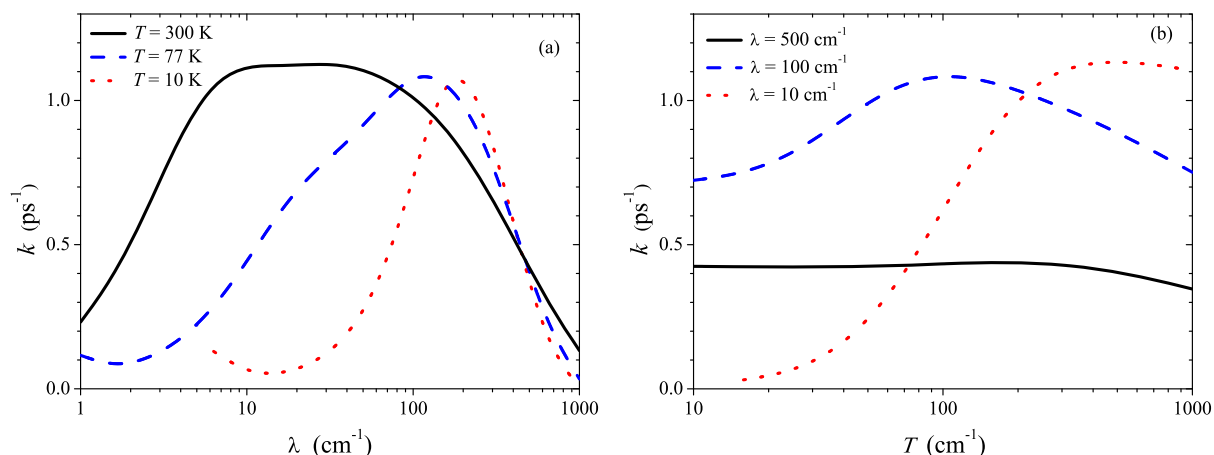


Figure 2. The transfer rate k , equation (3), in the absence of disorder as a function of (a) the reorganization energy λ for various values of the temperature $T = 300, 77$ and 10 K (solid, dashed and dotted), and (b) the temperature T for $\lambda = 500, 100$ and 10 cm^{-1} (solid, dashed and dotted).

agreement with experiment (1.25 ps^{-1}) [40]. Hence, comparing the donor B800 and acceptor B850 parameters, in calculating the rate for various disorder and bath coupling strengths below, we set $\lambda_A = 5\lambda$ and $\sigma_D = 0.2\sigma$. Treating the B800 ring as a monomer fails to capture the blue tail originating in the B800 intraring coherence [42]. Previous calculations of the B800–B850 EET rate [22–24, 42], both with and without disorder, have employed numerous theoretical approaches and parameterization schemes. Advances in single molecule spectroscopies continue to yield even finer detailed structural and dynamical information on pigment–protein complexes (site energies, electronic couplings, bath spectral densities, disorder characteristics, etc) [43, 44]. While we here employ the simplest of descriptions of the B800–B850 model and EET process, the essential *qualitative* dependence of the EET on the disorder and bath coupling strengths is captured, so that the major conclusions of this work remain intact.

2. Results

We begin by considering the optimal bath coupling strength in the absence of energetic disorder. In figure 2(a), the B800–B850 EET rate defined in equation (3) is plotted as a function of the reorganization energy λ (cm^{-1}), for various values of the temperature T (K). For all temperatures, the transfer rate exhibits a clear maximum as a function of the reorganization energy. This is directly due to the asymmetry of the system, i.e. the energy bias between 800 and 850 nm, allowing one to identify an optimal coupling strength. As temperature decreases, the range in coupling strength for which the rate is maximal narrows and shifts to stronger coupling. This can be understood as due to the severe narrowing of the spectra at low temperatures, so that increasingly strong coupling is required to broaden the spectra and achieve overlap. In figure 2(b), the temperature dependence of the transfer rate is shown for weak, intermediate and strong coupling, displaying a maximum in each case. However, as the coupling strength increases, the maximum shifts to lower temperatures, becoming less pronounced, indicating temperature insensitivity, so that the rate is almost temperature independent. We remark that

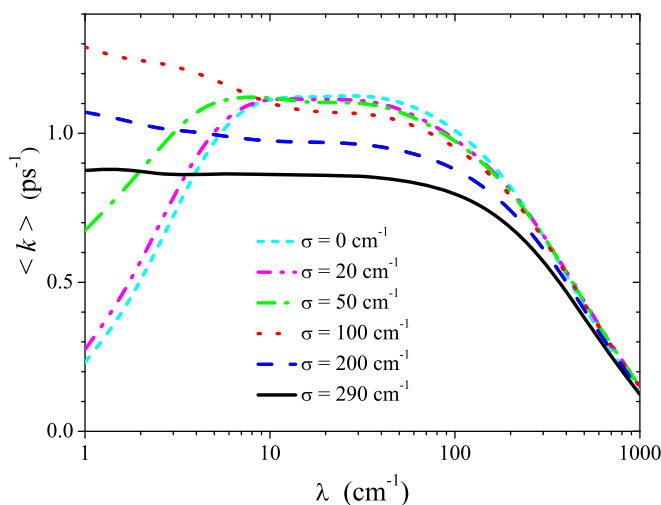


Figure 3. The average transfer rate $\langle k \rangle$ as a function of the reorganization energy for increasing strength of the static disorder, $\sigma = 20, 50, 100, 200$ and 290 cm^{-1} and $T = 300 \text{ K}$. The presence of disorder dramatically changes the profile, completely removing the maximum present in the ordered case (short dashed line).

at low temperatures *and* bath coupling strengths, where the exciton motion is almost entirely coherent, the MC-FRET theory itself (regardless of the IPR MC-FRET approach used here) is no longer valid, indicated by the truncated dashed and dotted curves in both figures 2(a) and (b). Further study of the disorder for a wide range in temperature and coupling could elucidate the observed temperature insensitivity [45]. Considering here only the physiologically relevant temperature $T = 300 \text{ K}$, we identify the optimal bath coupling strength in the absence of disorder as a weak to intermediate bath coupling strength $10 < \lambda < 100 \text{ cm}^{-1}$.

We next consider the effect of energetic disorder at room temperature. In figure 3 we plot the average transfer rate, as a function of the reorganization energy for increasing strength of the disorder at $T = 300 \text{ K}$. Upon increasing the disorder, the well-defined maximum transfer rate observed in the disorder-free rate is completely averaged out, yielding essentially monotonic average rate dependence (solid curve) at $\sigma = 290 \text{ cm}^{-1}$, so that we cannot easily identify an optimal bath coupling strength. Hence, the *average* rate is an insufficient optimization criterion. However, an additional important result is apparent in figure 3. Depending on λ , increasing the energetic disorder σ can either enhance or suppress the transfer rate (essentially enhancing the rate for weak coupling while suppressing for strong coupling). Thus, by reducing the eigenstate energy mismatch, resulting in increased spectral overlap, the disorder can assist the EET process. Furthermore, at weak coupling $\lambda < 10 \text{ cm}^{-1}$, the disorder *dramatically* enhances the transfer rate, so that $\langle k \rangle$ is highly sensitive to σ . This is in sharp contrast to the dependence around $\lambda \sim 200 \text{ cm}^{-1}$, where the disorder only *mildly* reduces the rate. Indeed, while the disorder ultimately removes the maximum of the disorder-free transfer rate (short dashed line), the average transfer rate $\langle k \rangle$ in this range remains largely unaffected, suggesting a robustness afforded at intermediate coupling strength.

To investigate further, in figure 4(a) we plot the probability density of the transfer rate for weak, intermediate and strong bath coupling strengths for a disorder strength of $\sigma = 290 \text{ cm}^{-1}$.

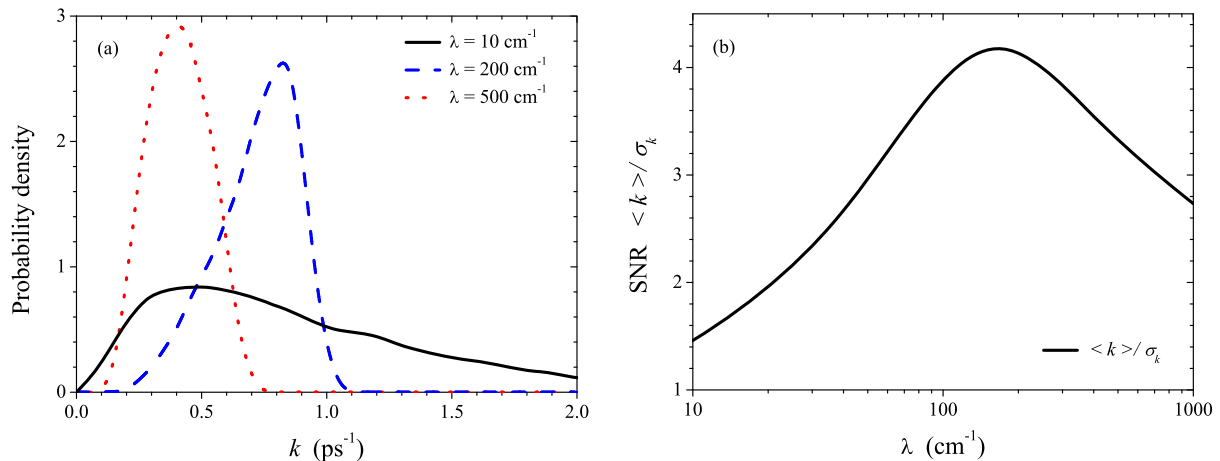


Figure 4. (a) The transfer rate probability density at $T = 300 \text{ K}$, for weak, intermediate and strong reorganization energy, $\lambda = 10, 200$ and 500 cm^{-1} , (solid, dashed and dotted) and a disorder of $\sigma = 290 \text{ cm}^{-1}$. (b) The relative disparity (SNR) $\langle k \rangle / \sigma_k$ as a function of λ . A maximal EET rate and minimal deviation, i.e. maximum relative dispersity (SNR), can be achieved as a function of coupling strength.

Immediately, one notes the significant standard deviation of the density σ_k for weak bath coupling (solid curve), due to the high sensitivity of the transfer rate to the disorder in this regime. This sensitivity is removed upon increasing the coupling, as evident from the narrowing distributions. However, increasing the coupling beyond $\lambda \sim 200 \text{ cm}^{-1}$ results in a reduced average rate as indicated by the shift in peaks. This observation is verified in figure 4(b), where the relative dispersity of the transfer rate or the SNR, defined as the ratio of the mean to the standard deviation (i.e. the inverse of the coefficient of variation), $\text{SNR} = \langle k \rangle / \sigma_k$, displays a maximum as a function of λ . In order to achieve efficient EET from B800 to B850 in LH2, a maximal transfer rate accompanied by a narrowed distribution of rates can be attained as a function of the bath coupling strength. In other words, there exists an optimal value of the bath coupling strength for achieving maximal EET rate and minimal deviation (high dispersity of rates), resulting in a maximal EET process robust to the effects of static disorder. This constitutes the principal result here reported.

3. Conclusions

We conclude the existence of an optimal bath coupling strength in LH2 for producing maximal B800–B850 EET and minimal deviation in order to achieve robust EET. While a fast average transfer rate is achieved at weak bath coupling, the high sensitivity to the disorder yields a very broad probability density, revealing a fragility of the transfer rate in this coupling regime. This fragility originates in the coherent dynamics at weak bath coupling, where the EET process is dominated by the energy bias and hence is sensitive to the disorder. By simply extending our optimization criterion beyond $\langle k \rangle$ to include the standard deviation σ_k , i.e. to the relative dispersity (i.e. SNR), we can consider this fragility. Hence, the fact that the relative disparity can be maximized as a function of the bath coupling strength has strong implications

for the interplay of coherent and incoherent dynamics in photosynthetic systems, suggesting that it is not optimal to promote fully coherent or incoherent transfer dynamics. Our results ultimately compound the importance of the interplay of coherent and incoherent dynamics in photosynthetic systems.

In summary, in order to investigate the existence of an optimal heat bath regime to facilitate EET from B800 to B850 in LH2, we have calculated the MC Förster rate, equation (3), for a wide range of the bath parameter space in the presence of energetic disorder. To achieve this, in addition to the diagonal approximation in the eigenstate basis, novel use of approximate expressions for the emission and absorption spectra, capable of capturing the essential qualitative behavior of the energy transfer process for a wide range of the reorganization energy λ , has been made. Our demonstration of an optimal coupling strength to achieve a maximum relative dispersity (i.e. SNR) has implications for understanding efficient EET and pigment–protein design. A future study that employs more rigorous calculation and detailed modeling of the B800–B850 EET rate can provide a better quantitative description of the maximized relative dispersity and hence determine more accurately the optimal coupling range. Indeed, inclusion of the B800 coherence, which enhances the average EET rate and narrows its distribution at room temperature [13, 42], is expected to re-enforce our finding.

Acknowledgments

This work was supported by the National Science Foundation (grant no. CHE-1112825) and DARPA (grant no. N99001-10-1-4063). LC is supported by the Center of Excitonics, an Energy Frontier Research Center funded by the US Department of Energy, Office of Science, Office of Basic Energy Sciences under Award no. DE-SC0001088. We thank T Pullerits, J Köhler and Y C Cheng for helpful comments.

Appendix A. LH2 model calculation details

Calculation of the IPR MC-FRET can be simplified by rewriting the integral in the time domain. Substituting equations (4) and (5) into equation (3) we have

$$k = \sum_{\mu=1}^{N_D} \sum_{\nu=1}^{N_A} \rho_{\mu}^{\text{st}} \frac{|J_{\mu,\nu}|^2}{\hbar^2} 2\Re \int_0^{\infty} e^{-i(\varepsilon_{\nu}-\varepsilon_{\mu}+N_{\mu}^D\lambda_D+N_{\nu}^A\lambda_A)t/\hbar} e^{-N_{\mu}^D g_D(t)-N_{\nu}^A g_A(t)} dt, \quad (\text{A.1})$$

where we have ultimately used the fact that $g(-t) = g^*(t)$. For the LH2 model calculation outlined above, we set $N_D = N_{\mu}^D = \rho_{\mu}^{\text{st}} = 1$ and $\lambda_A = 5\lambda_D$ so that we have

$$k = \sum_{\nu=1}^{18} \frac{|J_{1,\nu}|^2}{\hbar^2} 2\Re \int_0^{\infty} e^{-i(\varepsilon_{\nu}-E_D+\lambda+5N_{\nu}^A\lambda)t/\hbar} e^{-g(t)(1+5N_{\nu}^A)} dt, \quad (\text{A.2})$$

where we have noted that $\varepsilon_{\mu=1} = E_D$ and set $\lambda_D = \lambda$. For the Drude–Lorentz spectral density, the integral in the bath correlation function equation (6) can be evaluated via contour integration, so that the exact expression for the lineshape function is [27]

$$g(t) = \frac{\lambda}{\hbar\Lambda} (\cot(\beta\hbar\Lambda/2) - i) (e^{-\Lambda t} + \Lambda t - 1) + \frac{4\lambda\Lambda}{\beta\hbar^2} \sum_{q=1}^{\infty} \frac{(e^{-v_q t} + v_q t - 1)}{v_q(v_q^2 - \Lambda^2)}, \quad (\text{A.3})$$

where $v_q = 2\pi q/\beta\hbar$ are the Matsubara frequencies. In the high temperature limit $\beta\hbar\Lambda \ll 1$, equation (A.3) simplifies to

$$g(t) = \left(\frac{2\lambda}{\beta\hbar^2\Lambda^2} - i\frac{\lambda}{\hbar\Lambda} \right) (e^{-\Lambda t} + \Lambda t - 1). \quad (\text{A.4})$$

The intercomplex couplings J_{mn} are calculated using the point dipole approximation

$$J_{mn} = C \left(\frac{\vec{d}_m \cdot \vec{d}_n}{|\vec{r}_{mn}|^3} - \frac{3(\vec{r}_{mn} \cdot \vec{d}_n)(\vec{r}_{mn} \cdot \vec{d}_m)}{|\vec{r}_{mn}|^5} \right).$$

Here $\vec{d}_m = \langle 0 | \vec{d} | m \rangle$ and $\vec{d}_n = \langle 0 | \vec{d} | n \rangle$ are unit vectors describing the direction of the transition dipole moments of the donor and acceptor complexes, \vec{r}_{mn} is the vector connecting the centers (the M_g atom) of chromophore m and chromophore n , and C is an appropriate, dimensioned constant. The intracomplex couplings of the acceptor B850 ring (excluding the nearest neighbors) are calculated in identical manner. All coordinates were obtained from the protein data bank (ID code 1NKZ), with the transition dipole moments calculated from the N_B to N_D atom. The coordinates of the M_g atom of the single B800 chromophore used in the calculation were 28.62, 11.76 and 31.19 Å.

Appendix B. Slow and fast bath dynamics

The limiting cases of the line shape function $g(t)$ for slow bath (inhomogeneous broadening) and fast bath (homogeneous broadening) dynamics are easily obtained analytically in the high temperature approximation. In the limit of long bath correlation time $(\beta\hbar^2\Lambda^2/2\lambda)^{1/2} \ll 1$, the high temperature lineshape function equation (A.4) simplifies to $g(t) = \lambda t^2/\beta\hbar^2$ [27]. Substituting this expression into equations (4) and (5), we obtain the Gaussian emission and absorption spectra

$$E_\mu^D(\omega) = \rho_\mu^{\text{st}} \frac{\hbar}{\sqrt{4\pi N_\mu^D \lambda / \beta}} e^{-\beta(\varepsilon_\mu - N_\mu^D \lambda - \omega\hbar)^2 / 4N_\mu^D \lambda} \quad (\text{B.1})$$

and

$$I_v^A(\omega) = \frac{\hbar}{\sqrt{4\pi N_v^A \lambda / \beta}} e^{-\beta(\varepsilon_v + N_v^A \lambda - \omega\hbar)^2 / (4N_v^A \lambda)}. \quad (\text{B.2})$$

The above eigenstate spectra have a stokes shift of $N_{\mu,v}\lambda$, where we have introduced the sum of participation ratios $N_{\mu,v} = N_\mu^D + N_v^A$. Evaluating the overlap integral equation (3), we obtain the IPR MC-FRET rate in the slow bath limit

$$k = \sum_{\mu=1}^{N_D} \sum_{v=1}^{N_A} \frac{|J_{\mu,v}|^2}{2\pi} \rho_\mu^{\text{st}} \frac{e^{-\beta(N_{\mu,v}\lambda + \varepsilon_v - \varepsilon_\mu)^2 / 4N_{\mu,v}\lambda}}{\sqrt{4\pi N_{\mu,v}\lambda / \beta}}, \quad (\text{B.3})$$

The donor–acceptor transfer rates in equation (B.3) are formally identical to the Marcus rate of electron transfer except that the reorganization energy is scaled by a factor of $N_{\mu,v}$. In the case of a single donor and single acceptor chromophore $N_{\mu,v} \rightarrow 2$; recall that FRET assumes independent donor and acceptor baths, so that a factor of 2 appears in the bath coupling when compared to the Marcus rate, which assumes anti-correlated baths. In the opposite limit of short bath correlation time $(\beta\hbar^2\Lambda^2/2\lambda)^{1/2} \gg 1$, the high temperature lineshape function simplifies to

$g(t) = ((\beta\hbar\Lambda)^{-1} - i)\lambda t/\hbar$. Substituting this expression into equations (4) and (5), we obtain the Lorentzian emission and absorption spectra

$$E_{\mu}^{\text{D}}(\omega) = \rho_{\mu}^{\text{st}} \frac{1}{\pi} \frac{N_{\mu}^{\text{D}}\lambda}{N_{\mu}^{\text{D}2}\lambda^2/(\beta\hbar^2\Lambda) + (\varepsilon_{\mu} - \omega\hbar)^2\beta\Lambda}, \quad (\text{B.4})$$

$$I_{\nu}^{\text{A}}(\omega) = \frac{1}{\pi} \frac{N_{\nu}^{\text{A}}\lambda}{N_{\nu}^{\text{A}2}\lambda^2/(\beta\hbar^2\Lambda) + (\varepsilon_{\nu} - \omega\hbar)^2\beta\Lambda}. \quad (\text{B.5})$$

Note the absence of the Stokes shift between the spectra. The IPR MC-FRET rate in the fast bath limit is then

$$k = \sum_{\mu=1}^{N_{\text{D}}} \sum_{\nu=1}^{N_{\text{A}}} \frac{|J_{\mu,\nu}|^2}{2\pi} \frac{\rho_{\mu}^{\text{st}} N_{\mu,\nu} \lambda \beta \hbar^2 \Lambda}{\pi (N_{\mu,\nu}^2 \lambda^2 / (\beta \hbar^2 \Lambda)^2 + (\varepsilon_{\mu} - \varepsilon_{\nu})^2 / \hbar^2)}. \quad (\text{B.6})$$

Again in the case of a single donor and single acceptor chromophore, where $N_{\mu,\nu} \rightarrow 2$, it is easy to see that the rates in equation (B.6) are formally identical to the inverse exciton lifetime as yielded by the well-known Haken–Strobl model of a two-level system (the Haken–Strobl model assumes an infinite temperature bath, here equivalent to a high-temperature fast bath) [9].

References

- [1] Blankenship R E 2002 *Molecular Mechanisms of Photosynthesis* (London: Blackwell)
- [2] Engel G S, Calhoun T R, Read E L, Ahn T-K, Mancal T, Cheng Y-C, Blankenship R E and Fleming G R 2007 *Nature* **446** 782
- [3] Collini E, Wong C Y, Wilk K E, Curmi P M G, Brumer P and Scholes G D 2010 *Nature* **463** 644
- [4] Fleming G R, Huelga S F and Plenio M B 2011 *New J. Phys.* **13** 115002
- [5] Christensson N, Kauffmann H F, Pullerits T and Mancal T 2012 *J. Phys. Chem. B* **116** 7449
- [6] Tiwari V, Peters W K and Jonas D M 2013 *Proc. Natl Acad. Sci. USA* **110** 1203
- [7] Rebentrost P, Mohseni M, Kassar I, Lloyd S and Aspuru-Guzik A 2009 *New J. Phys.* **11** 033003
- [8] Caruso F, Chin A W, Datta A, Huelga S F and Plenio M B 2009 *J. Chem. Phys.* **131** 105106
- [9] Cao J and Silbey R J 2009 *J. Phys. Chem. A* **113** 13825
- [10] Escalante M, Lenferink A, Zhao Y, Tas N, Huskens J, Hunter C N, Subramaniam V and Otto C 2010 *Nano Lett.* **10** 1450
- [11] Pflock T J, Oellerich S, Krapf L, Southall J, Cogdell R J, Ullmann G M and Köhler J 2011 *J. Phys. Chem. B* **115** 8821
- [12] Cleary L, Chen H, Chuang C, Silbey R J and Cao J 2013 *Proc. Natl Acad. Sci. USA* **110** 8537
- [13] van Grondelle R and Novoderezhkin V I 2006 *Phys. Chem. Chem. Phys.* **8** 793
- [14] Harel E and Engel G S 2012 *Proc. Natl Acad. Sci. USA* **109** 706
- [15] Pullerits T, Chachisvilis M and Sundström V 1996 *J. Phys. Chem.* **100** 10787
- [16] Alden R G, Johnson E, Nagarajan V, Parson W W, Law C J and Cogdell R G 1997 *J. Phys. Chem. B* **101** 4667
- [17] Hu X, Ritz T, Damjanović A and Schulten K 1997 *J. Phys. Chem. B* **101** 3854
- [18] Wu J, Liu F, Ma J, Silbey R J and Cao J 2012 *J. Chem. Phys.* **137** 174111
- [19] Moix J, Wu J, Huo P, Coker D and Cao J 2011 *J. Phys. Chem. Lett.* **2** 3045
- [20] Wu J, Liu F, Shen Y, Cao J and Silbey R J 2010 *New J. Phys.* **12** 105012
- [21] Huo P and Coker D F 2010 *J. Chem. Phys.* **133** 184108
- [22] Sumi H 1999 *J. Phys. Chem. B* **103** 252
- [23] Scholes G D and Fleming G R 2000 *J. Phys. Chem. B* **104** 1854
- [24] Jang S, Newton M D and Silbey R J 2004 *Phys. Rev. Lett.* **92** 218301

- [25] Renger T and May V 2000 *Phys. Rev. Lett.* **84** 5228
- [26] Yang M 2005 *J. Chem. Phys.* **123** 124705
- [27] Mukamel S 1995 *Principles of Nonlinear Optical Spectroscopy* (New York: Oxford University Press)
- [28] Mukai K, Abe S and Sumi H 1999 *J. Phys. Chem. B* **103** 6096
- [29] Jang S, Newton M D and Silbey R J 2007 *J. Phys. Chem. B* **111** 6807
- [30] Cleary L and Cao J 2014 in preparation
- [31] Ma J and Cao J 2014 in preparation
- [32] Cho M, Vaswani H M, Brixner T, Stenger J and Fleming G R 2005 *J. Phys. Chem. B* **109** 10542
- [33] Renger T, May V and Kühn O 2001 *Phys. Rep.* **343** 137
- [34] McDermott G, Prince S M, Freer A A, Hawthornthwaite-Lawless A M, Papiz M Z, Cogdell R J and Isaacs N W 1995 *Nature* **374** 517
- [35] Strümpfer J and Schulten K 2009 *J. Chem. Phys.* **131** 225101
- [36] Pullerits T, Monshouwer R, van Mourik F and van Grondelle R 1995 *Chem. Phys.* **194** 395
- [37] Creemers T M H, De Caro C A, Visschers R W, van Grondelle R and Völker S 1999 *J. Phys. Chem. B* **103** 9770
- [38] Renger T and Marcus R A 2002 *J. Chem. Phys.* **116** 9997
- [39] Weiss U 2008 *Quantum Dissipative Systems* 3rd edn (Singapore: World Scientific)
- [40] Ma Y-Z, Cogdell R J and Gillbro T 1997 *J. Phys. Chem. B* **101** 1087
- [41] Strümpfer J and Schulten K 2011 *J. Chem. Phys.* **134** 095102
- [42] Cheng Y C and Silbey R J 2006 *Phys. Rev. Lett.* **96** 028103
- [43] Baier J, Richter M F, Cogdell R J, Oellerich S and Köhler J 2008 *Phys. Rev. Lett.* **100** 018108
- [44] Tubasum S, Cogdell R J, Scheblykin I G and Pullerits T 2011 *J. Phys. Chem. B* **115** 4963
- [45] Pullerits T, Hess S, Herek J L and Sundström V 1997 *J. Phys. Chem. B* **101** 10560